Remote control of liquid crystal elastomer random laser using external stimuli

# Remote control of liquid crystal elastomer random laser using external stimuli

Anjani Kumar Tiwari,[1,a)] Lorenzo Pattelli,[1] Renato Torre,[1,2] and Diederik S. Wiersma[1,2,3]
[1]*European Laboratory for Non-Linear Spectroscopy (LENS), University of Florence, via Nello Carrara 1, I-50019 Sesto Fiorentino, Italy*
[2]*Dip. di Fisica ed Astronomia, University of Florence, via G. Sansone 1, I-50019 Sesto Fiorentino, Italy*
[3]*Instituto Nazionale di Ricerca Metrogica (INRiM), Strada delle Cacce 91, I-10135 Torino, Italy*

(Received 4 May 2018; accepted 20 June 2018; published online 5 July 2018)

We present a distinct design for a random laser based on a composite material consisting of an elastomeric liquid crystal with embedded $TiO_2$ nanoparticles. Random lasing action can be controlled by an external, non-contact light stimulus; this induces a rearrangement of the elastomeric liquid crystals which moves the laser body in and out of the focal plane of a pump laser, pushing its emission above or below the lasing threshold. *Published by AIP Publishing.*
https://doi.org/10.1063/1.5038663

Random lasers are unique optical sources combining random scattering events with optical gain to provide coherent emission. Their ease of fabrication raises the demand for random lasers as attractive optical sources for various applications.[1] In the recent past, random lasing has been demonstrated in many kinds of materials such as dielectric nanopowders, dye-doped scatterers, and biological tissues.[2–9] In general, random lasers are non-linear open systems exhibiting an output signal characterized by strong fluctuations in emission frequencies, intensity, and the number of modes. For practical applications, a major drawback of a random laser is the limited controllability of its emission properties, which calls for the development of new strategies to control these fluctuations. Previous attempts to tackle this issue can be broadly classified into two categories which focus either on modulating the scattering mean free path of scatterers or on the control of the gain properties of the amplifying medium.[10–19] For example, monodisperse scatterers have been used to achieve wavelength-sensitive scattering.[10–14] The idea behind using monodisperse scatterers was to minimize the scattering mean free path at the resonant frequencies, resulting in wavelength-sensitive lasing at the resonances. In another case, the spatial distribution of the pump profile was optimized so as to have a particular random lasing mode undergoing preferential gain.[15–18]

The direct control of the lasing threshold and output intensity of a random laser has been successfully achieved in many systems. Among them, liquid crystal (LC) based random lasers offer distinctive features which can be directly exploited to tune the characteristics of output emission.[20–27] Typical examples regard the control of the alignment direction of the liquid crystals, e.g., by using electric fields,[20,21] which in turn can affect the orientation of dye molecules changing the quantum yield for different pump polarizations.[22] Other approaches exploit the temperature-dependent phase transition for modifying the scattering strength of the system and thus for bringing the random laser above and below its lasing threshold.[23,24] However, the physical motion of the random laser has never been considered to control or trigger the random lasing modes so far.

In this paper, we demonstrate random lasing in a composite system consisting of a transparent liquid crystal elastomer (LCE) body and a scattering tip with embedded $TiO_2$ nanoparticles in the presence of an amplifying medium. The composite LCE random laser is initially positioned in proximity of the focal plane of a pump laser. Using an external stimulus, the composite LCE can be moved in and out of the focal plane of the pump laser. When the composite LCE is in its resting position (out of the focal plane of the pump laser), the typical gain medium spectrum appears in the emission. However, when it moves towards the focal plane of the pump laser, a narrow bandwidth emission arises with a well-defined threshold. This makes it possible to control the emission of the composite random laser by inducing and exploiting its motion. Thus, the random lasing relies on self-actuating oscillation provided by the external stimuli.[28]

The composite random laser is made of two parts which are combined to form a single structure. For the fabrication of the LCE random laser, a thin layer of polyvinyl alcohol (PVA) is first spin-coated on the glass coverslip and then rubbed along the surface using a cotton texture. Another coverslip is spin-coated with a PI-1211 layer and placed to form a 200 μm-thick cell using calibrated spacers (monodisperse silica microspheres). The liquid crystal (LC) solution (79 mol. % LC monomer, 20 mol. % crosslinker, and 1 mol. % photoinitiator) containing $4 \times 10^{-3}$ M DCM dye is infiltrated by capillary action into the cell from one side.[29,30] The chemical structure of the liquid-crystalline monomer mixture used for our experiments is depicted in Fig. 1(a). The temperature of the mixture was maintained at 80 °C for 1 h. As illustrated in Fig. 1(b), the LC molecules transition from a homogeneous alignment (along the rubbing direction) near the PVA-coated surface to a homeotropic alignment near the PI-1211 layer. Overall, this results in an automatic splayed distribution of the LC molecules in the first half of the composite random laser. From the other side, we infiltrated LC solution containing DCM dye and the $TiO_2$ nanoparticles, which hinder the long-range alignment of LC molecules in the scattering half. However, local alignment is still possible

a)Electronic mail: tiwari.tifr@gmail.com

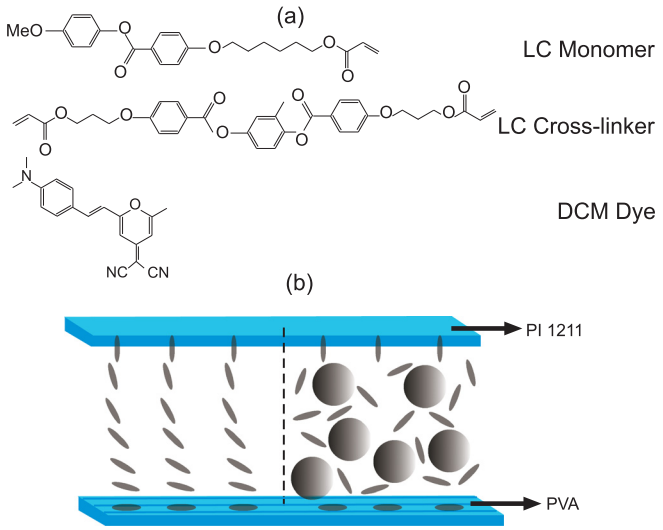


FIG. 1. (a) Chemical structure of the monomer, cross-linker, and dye molecule used to fabricate the composite random laser. (b) Schematic of the random laser: in the left half, the liquid crystals are aligned in the splayed fashion, and in the right half, the $TiO_2$ nanoparticles are dispersed to provide increased scattering.

in the vicinity of the sample surface. We then expose the mixture to UV radiation for 30 min, which cross-links and polymerizes the mixture in the described alignment structures, resulting in a single 200 μm-thick composite layer of LCE. The light transport mean free path of the LCE sample without $TiO_2$ was estimated using a coherent backscattering cone. The width of the backscattering cone was measured to be 0.095 mrad, corresponding to a scattering mean free path of around 735 μm. If we assume the 4 mM DCM dye molecules having a total inversion of the resonant state populations, the gain length of the sample will be ~40 μm. Thus, the critical thickness ($l_{cr} = \pi\sqrt{\frac{l_t l_g}{3}}$) for the random lasing sample under complete inversion is estimated to be around 310 μm. Hence, a pure LCE layer does not provide enough scattering to fully support the random lasing modes.[31] In the scattering region, we have the following parameters: the refractive index of the matrix medium is $n_{LCE} = 1.65$, the scattering nanoparticles have an average diameter $d$ of about 280 nm and a volume fraction $\phi$ of 0.005, a refractive index $n_{TiO_2} = 2.7$, a scattering anisotropy $g = 0.67$, and a scattering efficiency $Q_{scat} = 3.7$ which we estimated using Mie theory. According to these parameters, we obtain a scattering mean free path ($l_t = \frac{1}{1-g}(\frac{2d}{3\phi Q_{scat}})$) of about 30.5 μm assuming independent scattering given the very low volume fraction. Hence, this part of the composite supports random lasing.

If the size of the film is too large, the mechanical stress induced by the external stimulus can be less homogeneous, leading to a reduced deformation. Hence, following fabrication, we cut the composite film into several stripes about 2 mm wide and 1.5 cm long. The schematic of the experimental setup to move and simultaneously excite the composite LCE random laser is shown in Fig. 2(a). The light-driven bending in the elastomer stripe is induced by a 532 nm continuous wave laser (Coherent-Verdi 5W) chopped at a tunable rate, while the random lasing emission is excited by a pulse laser. The pulsed pump beam is generated using an amplified Nd:YAG laser system (EKSPLA-PL2143), with a

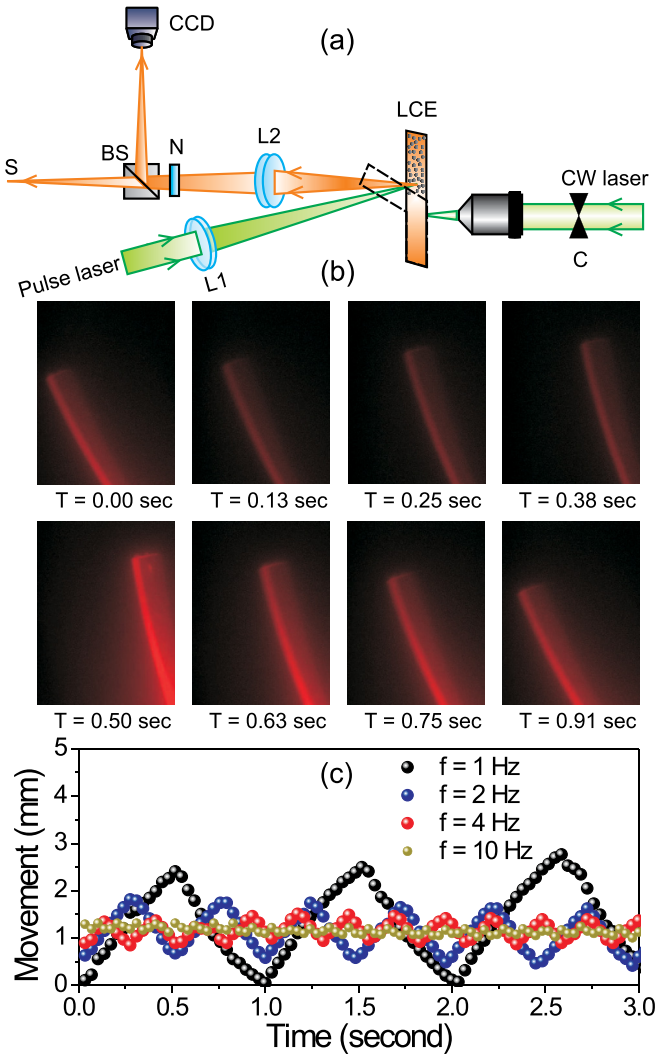


FIG. 2. (a) Schematic of the experimental setup to move and excite the random lasing modes in a composite LCE stripe. L1 and L2: lenses, N: notch filter, BS: beam splitter, C: chopper, and S: spectrometer. A chopped CW green laser actuates the LCE stripe, and the picosecond pulse laser triggers the random lasing emission. (b) Movement of the LCE stripe at $t = 0.0$, 0.13, 0.25, 0.38, 0.50, 0.63, 0.75, and 0.91 s. (c) Movement of the LCE stripe at actuating frequencies of 1 Hz, 2 Hz, 4 Hz, and 10 Hz. Multimedia views: https://doi.org/10.1063/1.5038663.1; https://doi.org/10.1063/1.5038663.2; https://doi.org/10.1063/1.5038663.3; https://doi.org/10.1063/1.5038663.4

pulse duration of 25 picoseconds ($\lambda = 532.8$ nm; rep. rate = 10 Hz). For optimal actuation of the LCE stripe, the CW laser was loosely focused using a 5× objective on the stripe (spot size ~200 μm), and the power was maintained at 7 W/mm$^2$. The top half of the LCE stripe is initially parked near the focal spot of 100 μm obtained by a 50 mm biconvex lens (L1) placed in the path of the pulsed laser beam. A 150 mm biconvex lens (L2) placed at 20° from the excitation axis collects the shot-to-shot emission spectra. A notch filter (N) was placed between lens L2 and the beam splitter (BS) to block the scattered green light. The beam splitter allows the simultaneous measurement of the motion of LCE and its spectral response. A high-resolution CCD camera operating at 29 frames/seconds was placed to monitor the movement of the LCE, while the spectra were analyzed with a 0.5 m spectrometer (S) having a spectral resolution of 0.1 nm.

When the LCE stripe is exposed to the actuating laser, the elastomer material expands locally in the direction

perpendicular to the molecular alignment. In the case of unidirectional alignment, this would result in a contraction along the liquid crystal director and an expansion along the other two directions. For a splay-aligned stripe, conversely, the two opposite sides undergo opposite deformations, inducing a mechanical stress which eventually results in an overall bending movement. Figure 2(b) shows a light-driven movement of the LCE random laser captured at a speed of 30 frames per second. At $t = 0$ s, the LCE stripe is at rest. As soon as the LCE stripe starts to feel the actuation laser, it starts to bend away from the objective. At $t = 0.5$ s, the top part of the structure reaches the maximum displacement from its rest position of around 2.5 mm (Multimedia view). Once the chopper blade obstructs the laser beam, the LCE stripe relaxes back to its initial position. The bending of the composite structure follows the chopper frequency with a small delay. Figure 2(c) shows the actuating response of the top portion of the LCE stripe at four actuating frequencies of 1 Hz, 2 Hz, 4 Hz, and 10 Hz. At 1 Hz actuation (black curve), the top part of the stripe undergoes a maximum displacement of 2.5 mm from its rest position. At 2 Hz (blue curve) and 4 Hz (red curve), the maximum displacement was found to be around 1.5 mm and 0.4 mm, respectively. When the chopping frequency of the CW laser is further increased to 10 Hz (green curve), the overall displacement of the tip decreases significantly and eventually becomes insignificant at larger repetition rates as the LCE stripe cannot undergo a full excitation-relaxation cycle in between subsequent actuation cycles. The extent of the movement/bend also depends on LCE stripe size and CW laser power. It is worth noting that the dynamics of LCE systems can be much faster on the microscale, where full actuation cycles have been demonstrated up to few hundred Hz.[32]

To show that the scattering part of the composite LCE laser is capable of supporting the random lasing modes, we first park the LCE stripe near the focal spot of the pulsed laser. The CW laser is not switched on, and thus, the actuation in the LCE stripe has not yet initiated. Figure 3(a) depicts the representative emission spectrum at increasing pump energies $E_p = 1.1$ μJ, 3.1 μJ, and 15.2 μJ per pulse. The spectra at $E_p = 3.1$ μJ and 15.2 μJ are scaled by a factor of 0.5 and 0.1, respectively. At smaller pump energy, the emission spectrum from the LCE stripe resembles the typical fluorescent profile of DCM dye. As the pumping energy increases, the output intensity starts to grow rapidly, and the emission profile narrows down. Figure 3(b) shows the output intensity and bandwidth of emission as a function of input pump energy averaged over 100 spectra. The lasing threshold for the composite random laser occurs at $E_{th} = 3.1$ μJ, above which the emission intensity grows abruptly and the bandwidth collapses to about 15 nm. These observations confirm the excitation of random lasing modes in the scattering region of the composite LCE stripe. Figure 3(c) shows typical emission spectra from the scattering LCE region when the actuation in the LCE stripe is switched on. Away from the focal plane, the emission spectra from the system resemble the typical emission profile of DCM dye molecules (as shown by the first few black curves). The left inset depicts the image of the emission spot, exhibiting a mild intensity, which further confirms that the lasing action has not set off

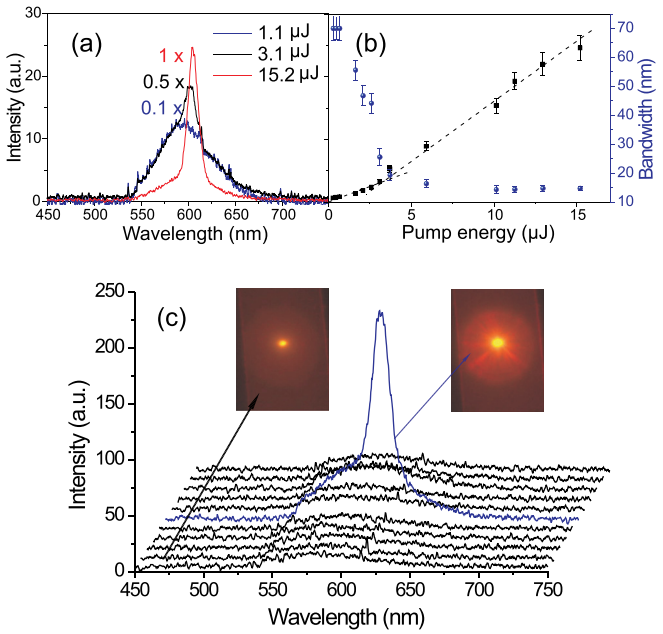


FIG. 3. (a) Single-shot emission spectrum from the LCE random laser at pump energies $E_p = 1.1$ μJ, 3.1 μJ, and 15.2 μJ. (b) Plot of the output intensity and FWHM of emission as a function of input pump energy shows the threshold for lasing at $E_{th} = 3.1$ μJ in the LCE laser. Error bars correspond to the standard deviations for 100 independent acquisitions. (c) Emission spectra from the actuated LCE stripe: black curves: when the stripe is away from the focal plane of the pulsed laser and blue curve: when the stripe is near the focal plane. The inset shows the corresponding image of the emission spot.

in the stripe. As the actuating LCE stripe approaches the focal plane of the pulsed laser, the emission intensity increases gradually. Near the focal plane, the dye molecules embedded in the LCE stripe experience a significant inversion. At this instant, the emission intensity shoots up by a factor of 20, and the bandwidth collapses to about 15 nm. The inset on the right side shows the emission spot which is visibly much brighter compared to the previous scenario. These observations again confirm the excitation of lasing modes from the moving composite LCE random laser. Once the actuating stripe moves away from the focal plane of the pulsed laser, the random lasing disappears, and the system again exhibits a typical emission profile of DCM dye molecules. The actuated LCE random laser periodically shows this dynamical behavior. Different realizations of LCE stripes do consistently show lasing action when positioned at the focal plane of the pump laser. During motion, on the other hand, the lasing intensity is affected by whether the ps laser pulse hits the LCE stripe at the right instant. The output intensity is maximum if the stripe is at the focal plane of the ps pump. In our experiment, the depth of focus is about 600 μm. Whenever the random lasing tip of the stripe moves within the depth of focus of the ps laser, we observe consistent lasing action for all actuation rates from 1 to 10 Hz.

In conclusion, we have demonstrated random lasing in a composite system consisting of liquid crystal elastomeric molecules with externally added scatters. The random lasing action in LCE is being switched on/off by inducing a noncontact controlled motion using an external optical stimulus. The optical excitation triggers a controllable and reversible movement in the elastomeric material, which drives the gain of the random laser medium in/out from the critical threshold

region and therefore allows us to control its emission. The remotely controlled elastomer random laser may be useful for light sensing, temperature sensing, and as an optical source for microchip devices. Moreover, a moving random laser architecture can overcome issues such as quenching or heating to increase its operational lifespan, and it is potentially compatible with self-actuating feedback mechanisms.

This work received funding from the European Research Council under the European Union's Seventh Framework Program (No. FP7/2007-2013)/ERC Grant Agreement No. 291349 on photonic microrobotics and partially founded by Ente Cassa di Risparmio Firenze, Prog. No. 2016-0866 and Laserlab-Europe, H2020 EC-GA (654148). We thank the entire Optics of Complex Systems group at LENS for the feedback and discussions. We also acknowledge Paolo Bartolini and Andrea Taschin for their valuable support.

[1]D. S. Wiersma, Nat. Phys. **4**, 359 (2008).
[2]*Solid-State Random Lasers*, edited by M. A. Noginov (Springer, New York, 2005).
[3]H. Cao, Y. G. Zhao, S. T. Ho, E. W. Seelig, Q. H. Wang, and R. P. H. Chang, Phys. Rev. Lett. **82**, 2278 (1999).
[4]H. Cao, "Lasing in random media," in *Waves in Random and Complex Media* (IOP Publishing, 2003), Vol. 13, pp. R1–R39.
[5]J. Fallert, R. J. B. Dietz, J. Sartor, D. Schneider, C. Klingshirn, and H. Kalt, Nat. Photonics **3**, 279 (2009).
[6]S. Mujumdar, M. Ricci, R. Torre, and D. S. Wiersma, Phys. Rev. Lett. **93**, 053903 (2004).
[7]S. K. Turitsyn, S. A. Babin, A. E. El-Taher, P. Harper, D. V. Churkin, S. I. Kablukov, J. D. Ania-Castanon, V. Karalekas, and E. V. Podivilov, Nat. Photonics **4**, 231 (2010).
[8]R. C. Polson and Z. V. Vardeny, Appl. Phys. Lett. **85**, 1289 (2004).
[9]S. Caixeiro, M. Gaio, B. Marelli, F. G. Omenetto, and R. Sapienza, Adv. Opt. Mater. **4**, 998 (2016).
[10]S. Gottardo, R. Sapienza, P. D. García, A. Blanco, D. S. Wiersma, and C. López, Nat. Photonics **2**, 429 (2008).
[11]R. Uppu and S. Mujumdar, Opt. Express **19**, 23523 (2011).
[12]A. K. Tiwari, R. Uppu, and S. Mujumdar, Photonics Nanostruct. Fundam. Appl. **10**, 416 (2012).
[13]A. K. Tiwari and S. Mujumdar, Phys. Rev. Lett. **111**, 233903 (2013).
[14]A. K. Tiwari, K. S. Alee, R. Uppu, and S. Mujumdar, Appl. Phys. Lett. **104**, 131112 (2014).
[15]N. Bachelard, J. Andreasen, S. Gigan, and P. Sebbah, Phys. Rev. Lett. **109**, 033903 (2012).
[16]B. N. S. Bhaktha, X. Noblin, N. Bachelard, and P. Sebbah, Appl. Phys. Lett. **101**, 151101 (2012).
[17]M. Leonetti, C. Conti, and C. Lopez, Nat. Photonics **5**, 615–617 (2011).
[18]M. Leonetti and C. Lopez, Appl. Phys. Lett. **102**, 071105 (2013).
[19]R. G. S. El-Dardiry and A. Lagendijk, Appl. Phys. Lett. **98**, 161106 (2011).
[20]Q. Song, L. Liu, L. Xu, Y. Wu, and Z. Wang, Opt. Lett. **34**(3), 298–300 (2009).
[21]C.-R. Lee, J. De Lin, B.-Y. Huang, S.-H. Lin, T.-S. Mo, S.-Y. Huang, C.-T. Kuo, and H.-C. Yeh, Opt. Express **19**, 2391–2400 (2011).
[22]G. Strangi, S. Ferjani, V. Barna, A. De Luca, C. Versace, N. Scaramuzza, and R. Bartolino, Opt. Express **14**, 7737 (2006).
[23]D. Wiersma and S. Cavalieri, Nature (London) **414**, 708–709 (2001).
[24]D. S. Wiersma and S. Cavalieri, Phys. Rev. E **66**, 056612 (2002).
[25]C.-R. Lee, J.-D. Lin, B.-Y. Huang, T.-S. Mo, and S.-Y. Huang, Opt. Express **18**, 25896 (2010).
[26]C.-R. Lee, S.-H. Lin, C.-H. Guo, S.-H. Chang, T.-S. Mo, and S.-C. Chu, Opt. Express **18**, 2406 (2010).
[27]Q. Song, S. Xiao, X. Zhou, L. Liu, L. Xu, Y. Wu, and Z. Wang, Opt. Lett. **32**, 373–375 (2007).
[28]K. Kumar, C. Knie, D. Bleger, M. A. Peletier, H. Friedrich, S. Hecht, D. J. Broer, M. G. Debije, and A. P. Schenning, Nat. Commun. **7**, 11975 (2016).
[29]H. Zeng, D. Martella, P. Wasylczyk, G. Cerretti, J.-C. G. Lavocat, C.-H. Ho, C. Parmeggiani, and D. S. Wiersma, Adv. Mater. **26**, 2319–2322 (2014).
[30]H. Zeng, P. Wasylczyk, G. Cerretti, D. Martella, C. Parmeggiani, and D. S. Wiersma, Appl. Phys. Lett. **106**, 111902 (2015).
[31]D. S. Wiersma and A. Lagendijk, Phys. Rev. E **54**, 4256 (1996).
[32]H. Zeng, P. Wasylczyk, C. Parmeggiani, D. Martella, M. Burresi, and D. S. Wiersma, Adv. Mater. **27**, 3883–3887 (2015).